Further investigation on the dynamic compressive strength enhancement of concrete-like materials based on split Hopkinson pressure bar tests Part I: Experiments

M. Zhang, H.J. Wu, Q.M. Li, F.L. Huang

Accepted Manuscript

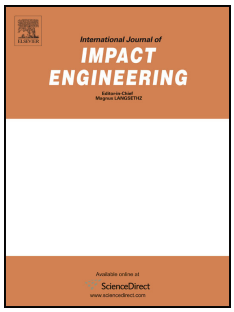

Title: Further investigation on the dynamic compressive strength enhancement of concrete-like materials based on split Hopkinson pressure bar tests Part I: Experiments

Authors: M. Zhang, H.J. Wu, Q.M. Li, F.L. Huang

PII: S0734-743X(09)00095-5

DOI: 10.1016/j.ijimpeng.2009.04.009

Reference: IE 1782

To appear in: *International Journal of Impact Engineering*

Received Date: 1 April 2008

Accepted Date: 17 April 2009

Please cite this article as: Zhang M, Wu HJ, Li QM, Huang FL. Further investigation on the dynamic compressive strength enhancement of concrete-like materials based on split Hopkinson pressure bar tests Part I: Experiments, International Journal of Impact Engineering (2009), doi: 10.1016/j.ijimpeng.2009.04.009

Further investigation on the dynamic compressive strength enhancement of concrete-like materials based on split Hopkinson pressure bar tests

Part I: Experiments

M.Zhang[1], H.J.Wu[1], Q.M.Li*[1,2] F.L.Huang[1]

[1] State Key Laboratory of Explosion Science and Technology
Beijing Institute of Technology, Beijing 100081, P.R.China

[2] School of Mechanical, Aerospace and Civil Engineering
The University of Manchester, PO Box 88, Manchester M60 1QD, UK

Abstract: Effects of the inertia-induced radial confinement on the dynamic increase factor (DIF) of a mortar specimen are investigated in split Hopkinson pressure bar (SHPB) tests. It is shown that axial strain acceleration is unavoidable in SHPB tests on brittle samples at high strain-rates although it can be reduced by the application of a wave shaper. By introducing proper measures of the strain-rate and axial strain acceleration, their correlations are established. In order to demonstrate the influence of inertia-induced confinement on the dynamic compressive strength of concrete-like materials, tubular mortar specimens are used to reduce the inertia-induced radial confinement in SHPB tests. It is shown that the DIF measured by SHPB tests on tubular specimens is lower than the DIF measured by SHPB tests on solid specimens. This paper offers experimental support for a previous publication [Li and Meng(2003), Int. J. of Solids and Struct., 40, 343-360], which claimed that inertia-induced radial confinement makes a large contribution to the dynamic compressive strength enhancement of concrete-like materials when the strain-rate is greater than a critical transition strain-rate between 10^1 and 10^2 s^{-1}. It is concluded that DIF formulae for concrete-like materials measured by split Hopkinson pressure bar tests need to be corrected if they are going to be used as the unconfined uniaxial compressive strength in the design and numerical modelling of structures made from concrete-like materials to resist impact and blast loads.

Keywords: concrete-like materials, split Hopkinson pressure bar, dynamic increasing factor, compressive strength, experimental study

*Corresponding author and guest professor to Beijing Institute of Technology; e-mail: qingming.li@manchester.ac.uk

1. Introduction

The dynamic increase factor (DIF), defined as the ratio of the dynamic strength to the quasi-static strength in uniaxial compression, has been widely accepted as an important parameter to measure the strain-rate effect on the compressive strength of concrete-like materials. Numerous experiments have been performed using various experimental techniques to characterize the DIF of concrete-like materials at strain-rates from 10^0 to 10^3 s^{-1}. A critical review was given by Bischoff and Perry (1991) to compare DIFs of concrete and mortar specimens from experiments conducted between 1910 and 1990. It clearly demonstrated the increase of DIF with strain-rate for concrete and mortar specimens although great discrepancies were observed due to differences in material and dimensions of the specimen and the method used in testing and measurement.

Among all available testing methods for dynamic compressive strength of concrete-like materials, the split Hopkinson pressure bar (SHPB), proposed originally by Kolsky (1949), has been used widely to measure the DIF of concrete-like materials at strain-rates between 10^1 to 10^3 s^{-1} since the 1980s. Based on studies of the applications of the SHPB to the dynamic behaviours of some metals and polymers, Davies and Hunter (1963) proposed an optimum dimension for the SHPB specimen, i.e. $L/D = \frac{1}{2}\sqrt{3\nu_s}$ where ν_s is Poisson's ratio and L and D are the length and the diameter of the specimen, respectively, in order to reduce the effects of inertia and friction on the measured dynamic stress in the specimen. Such optimal dimension is also adopted in SHPB tests for concrete-like materials (e.g. mortar, concrete, geo-material, ceramic etc.) [e.g. Grote et al (2001)]. However, researches have suggested that inertia effect cannot in general be cancelled by adjusting specimen geometry [Gorham et al (1984, 1992), Gorham(1991, 1992)], which indicates that the inertia effect need to be checked carefully at high strain-rates, especially in SHPB tests for brittle materials where large diameter specimens are used. Based on SHPB tests, DIFs of concrete-like materials have been studied extensively to obtain many empirical formulae, represented by CEB formula [Comite Euro-International du Beton (1993)] for concrete. It is interesting to note that all experimental data on the variation of DIF with strain-rate clearly demonstrate the existence of a critical transition strain-rate, beyond which the dependence of DIF on strain-rate becomes significant. This transition strain-rate varies in different testing set-ups, i.e. 30 s^{-1} in CEB formulae [Comite Euro-International du Beton (1993)], 63.1 s^{-1} in Ross's publications [Ross et al (1989, 1995, 1996), Tedesco and Ross(1998)] and 266 s^{-1} in Grote et al.(2001).

Based on a numerical study, Li and Meng(2003) demonstrated that the significant increase of DIF with strain-rate beyond the transition strain-rate is mainly due to the inertia-induced radial confinement effects. The dependence of the compressive strength of concrete-like materials on radial confinement had already been shown in confined quasi-static tests and strength models (e.g. Drucker-Prager model) and confined dynamic tests and analyses [e.g. Chen and Ravichandran(1997), Nemat-Nasser and Horii(1982), Huang et al.(2002), Huang et al.(2003)]. It was pointed out in Li and Meng(2003) that the misinterpretation of the confinement enhancement as the strain-rate enhancement in a SHPB test leads to non-conservative design or analysis of a concrete structure against impact or blast loading. It should be noted that a similar point of view has been indicated in other publications [e.g. Brace and Jones (1971), Gorham (1989), Gorham (1991), Bischoff and Perry (1991), Donze et al.(1999), Field et al.(2004)]. Forrestal et al.(2007) recently suggested a method to investigate the effect of the axial strain acceleration on the additional axial stress and radial confinement in a brittle cylindrical sample, which further support the previous findings on SHPB tests of concrete-like materials in Li and Meng(2003). The radial stress induced by axial strain acceleration in an elastic cylinder is given by [Forrestal et al.(2007)]

$$\sigma_r = \sigma_r^{'} = -\frac{\nu(3-2\nu)}{8(1-\nu)}\left[r^2 - b^2\right]\rho\ddot{\varepsilon}_z^0(t) \qquad (1)$$

where b is the radius of the cylindrical specimen, ν and ρ are the Poisson's ratio and the density of the specimen material, respectively; $\ddot{\varepsilon}_z^0(t)$ is the axial strain acceleration in the specimen. Equation (1) shows that the radial stress is influenced by two factors, i.e. the radius of the specimen and the axial strain acceleration in the specimen. The maximum radial stress occurs at the centre of the cross-section of the cylinder and reduces to zero on the outer surface of the cylinder according to a parabolic function. Unfortunately, the effect of the radial confinement on the measurement of DIF of concrete-like materials in dynamic compressive tests has been largely ignored by the users of the DIF data and formulae, which were derived mainly from SHPB tests. Many recent publications still employ DIF data and formulae as the dynamic compressive strength in uniaxial stress state to define the strain-rate effect on the compressive strength of concrete-like materials in corresponding constitutive models [e.g. Barpi(2004), Tham(2006), Katayama et al(2007), Polanco-Loria et al(2008)]. Similar recommendations also appeared in recent concrete model (K&C model) in LS-DYNA Version 971. The applications of the

misinterpreted DIF in the design and numerical simulation may cause significant increase of the predicted impact or blast resistance of structures made from concrete-like materials, and thus, lead to dangerous non-conservative design or assessment of these structures against impact and blast loads.

In the present paper, experimental evidences based on SHPB tests on solid and tubular mortar specimens are given to demonstrate the correlations between the representative axial strain-rate and the axial strain acceleration in a SHPB test on concrete-like material. A tubular specimen is introduced in order to reduce the inertia-induced radial confinement, and thus, demonstrate the influence of the inertial-induced radial confinement on DIF in SHPB tests, which further confirms the findings in Li and Meng(2003). Experiments are described in Section 2, which is followed by data analyses in Section 3 and discussion and conclusions in Sections 4 and 5.

2. Descriptions of Experiment

2.1. SHPB set-up

Series of experiments of solid and tubular specimens with different diameters (37mm, 50mm and 74mm) were tested at various strain-rates from 50 to 400 s^{-1} on a SHPB system (Fig.1). A gas gun was used to shoot the striker bar. The velocity of the striker bar, which is controlled by gas pressure, is measured by two parallel light gates and an electronic time counter. The signals from the strain gauges on the incident and transmitted pressure bars are amplified and then recorded by a transient recorder. Wave shaper is used in order to reduce the stress non-equilibrium in specimen.

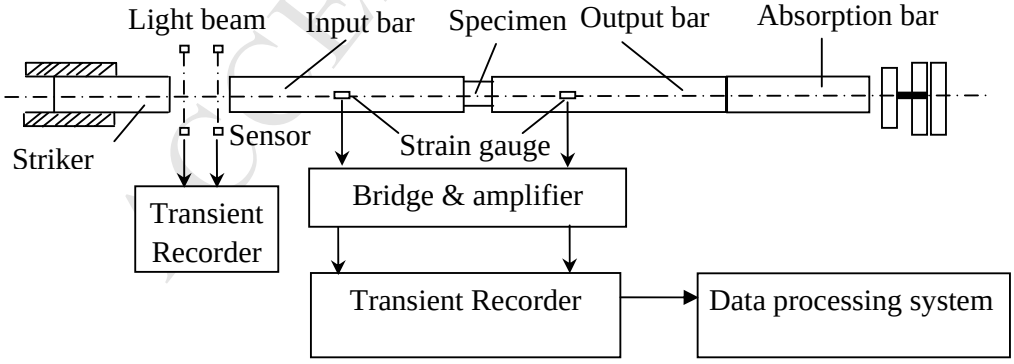

Fig.1 The schematic diagram of a SHPB set-up

2.2 SHPB specimen

The SHPB specimens are made of mortar which is a mixture of cement, water and medium fine sand. The mass ratio of the three materials is 533:302:1600. Typical solid and tubular specimens are shown in Fig.2. Dimensions of the specimen are shown by the specimen code, e.g. a specimen with code LT-aa-bb-cc-dd contains following information, (i) if T=S, it is a solid cylinder with outer diameter "aa", length "bb", inner diameter "cc"="00" and testing number "dd"; (ii) if T=H, it is a tubular cylinder with outer diameter "aa", length "bb", inner diameter "cc" and testing number "dd". "L" is a letter used for internal reference. The quasi-static mechanical properties of the mortar are given in Table 1.

(a) Solid SHPB specimen

(b) Tubular SHPB specimen

Fig.2 Typical solid and tubular SHPB specimens

Table 1 Mechanical properties of mortar

Specimen diameter (mm)	Density ρ (kg/m^3)	Unconfined uniaxial Compression strength f_c (MPa)	Young's modulus E (GPa)	Poisson's ratio μ
74.0	2179.0	44.9	17.2	0.19
37.0 & 50.0	2116.0	51.0	23.1	0.19

Typical signals obtained from strain gauges on incident and transmitted bars are shown in Fig.3. A thin rubber ring is used as the wave shaper. A wave shaper has two functions: (i) the achievement of stress equilibrium and (ii) the achievement of nearly constant strain-rate (i.e. nearly zero axial strain acceleration) in the SHPB specimen. The first requirement is satisfied by increasing the rise time of the input pulse through a wave shaper. But the second requirement is not satisfied in the present SHPB tests although the use of a wave shaper generally reduces the axial strain acceleration in the mortar specimen in SHPB test. The design of a proper wave shaper to meet the nearly constant strain-rate requirement is not always straightforward because it is

strongly depends on good matching between the dynamic properties of the wave shaper material and the tested material as well as their geometrical dimensions [e.g. Frew et al(2002)]. It will be shown in Section 3 that the axial strain acceleration increases with strain-rate in the present SHPB tests. Typical incident stress pulses obtained at different impact velocities in the present SHPB tests are shown in Fig.4. The duration of the incident stress pulse is nearly a constant determined by the length of the striker. However, the amplitude of the incident stress pulse increases linearly with the impact velocity of the striker, as shown in Fig.5. The incident stress pulse can be expressed by Eqs.(2, 3) using data-fitting method, i.e.

$$\sigma = \sigma_i \cdot \frac{1}{1+e^{-\frac{t-120}{12}}} \cdot \left(1 - \frac{1}{1+e^{-\frac{t-274}{12}}}\right) \tag{2}$$

where t (in μs) is time. σ_i is the amplitude of the incident stress, which increases linearly with the impact velocity of the striker, v_i (in m/s) , i.e.

$$\sigma_i = 20.6 v_i - 7.9 \quad \text{for 37mm SHPB} \tag{3a}$$

and

$$\sigma_i = 9.2 v_i - 16.0 \quad \text{for 74mm SHPB.} \tag{3b}$$

Equations (2) and (3) are only suitable for the present SHPB system and will be used in the companion numerical analysis in Li et al.(2009).

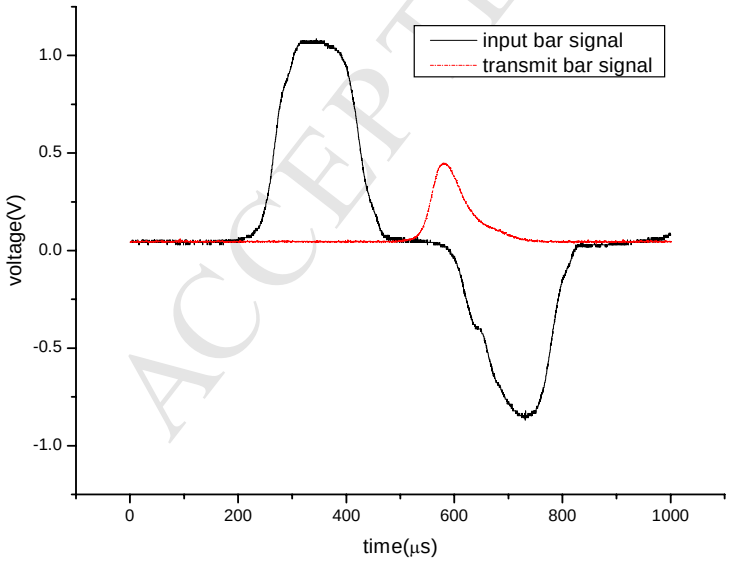

Fig.3 Typical strain gauge signals obtained from incident and transmitted pressure bars when wave shaper is applied

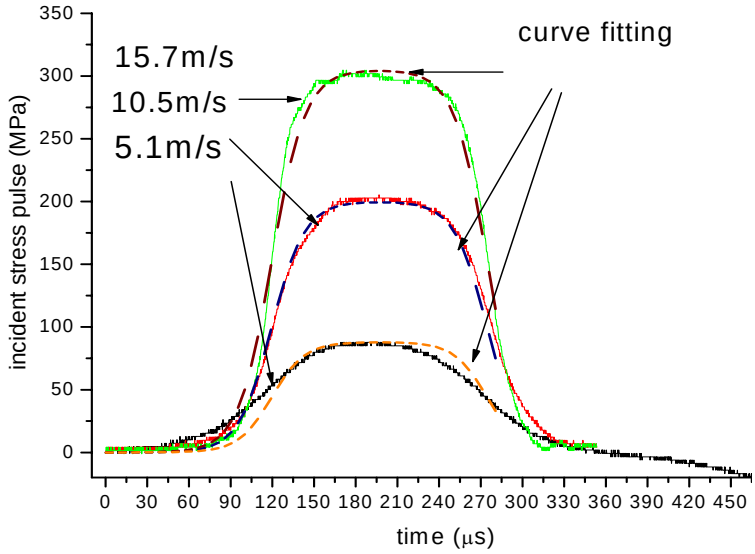

Fig.4 Typical incident stress pulses for different impact velocities

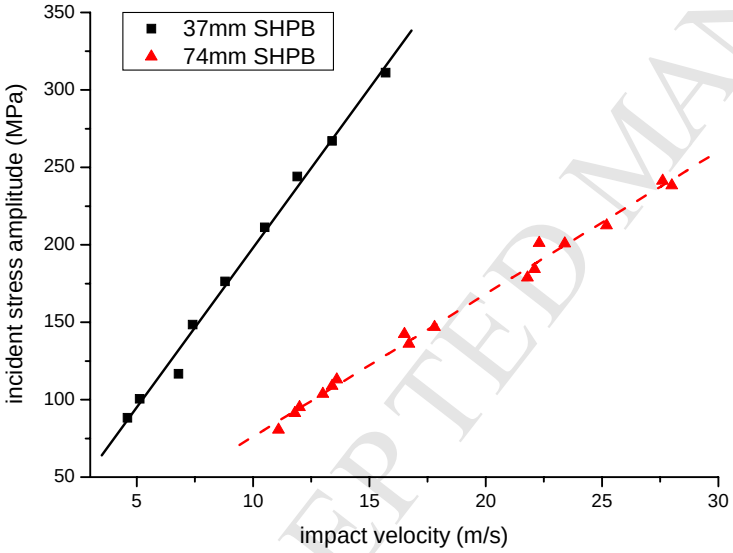

Fig.5 Variations of the incident stress amplitude and the impact velocity of the striker for 37mm and 74mm SHPBs

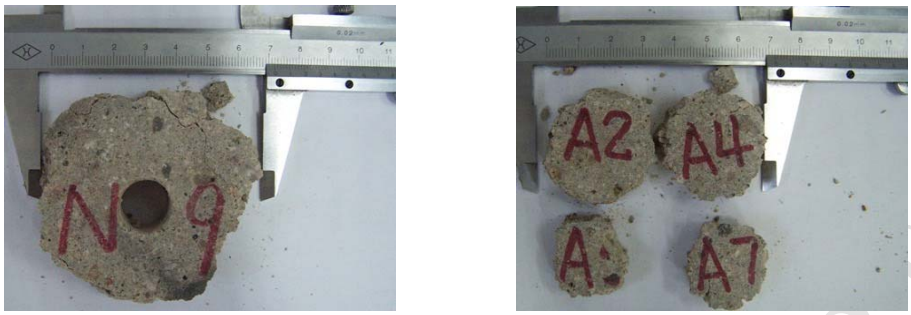

Fig.6 Recovered specimens after SHPB test

The recovered specimens after SHPB tests are shown in Fig.6. Spalling fragments and the longitudinal cracks are observed in the recovered specimens. The spalling fragments are almost axisymmetrically formed from the outer surface toward the centre of the specimen. An intact core is left if the specimen is not totally smashed, which implies that the central part of the specimen can resist large compressive loads.

The voltage signals measured in each SHPB test are processed according to the 3-wave formulae [Gray III (2000)] to obtain the variations of the engineering stress, strain and strain-rate with time as well as the engineering stress-strain relation. The formulae show that stress equilibrium in the SHPB specimen in each SHPB test is satisfied. Values of the dynamic longitudinal compressive strength at various strain-rates are obtained. These will be further discussed in Section 3.

3. Data analysis

3.1 Axial strain acceleration

The instantaneous average strain-rate in the specimen is obtained based on one-dimensional elastic stress wave theory

$$\dot{\varepsilon}_s(t) = \frac{v_1(t) - v_2(t)}{l_0} = \frac{c}{l_0}\left(\varepsilon_i - \varepsilon_r - \varepsilon_t\right) \quad . \tag{4}$$

The variations of strain-rate with time for solid specimens tested on a 74mm diameter SHPB at different impact velocities are shown in Fig.7. The figure shows that strain-rate during the effective loading period cannot be treated as a constant, especially when the impact velocity is increased to achieve high strain-rate. The gradient of the strain-rate curve in Fig.7, i.e. the axial strain acceleration, increases with impact velocity. Since the DIF measured in each SHPB test is

associated with a representative strain-rate, it is necessary to give a clear definition of such representative strain-rate used in SHPB tests. Usually, such representative strain-rate is defined as the mean value of the strain-rate over the loading period [e.g. Grote et al.(2001)]. Since mortar is a type of brittle material and most of the loading period is in the elastic deformation stage, the mean strain-rate during the loading period in a SHPB test is less relevant to the compressive failure of the specimen than the strain-rate at the failure point. Therefore, the strain-rate at the failure point, i.e. the end of the strain-rate curve in Fig.7, is used as the representative strain-rate in a SHPB test in the present paper. However, linear correlations between the strain-rate at the failure point and the mean strain-rate are revealed for all SHPB tests in the present study, e.g. Fig.8 for 74mm diameter SHPB tests on solid specimens.

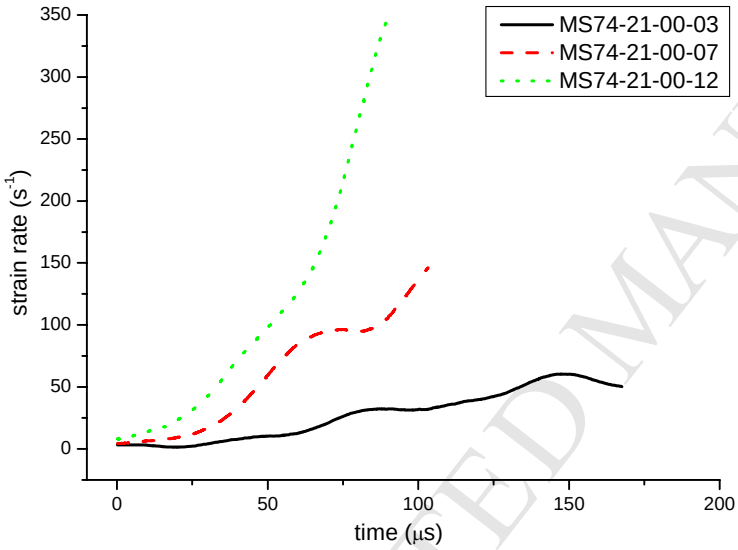

Fig.7 Variations of strain-rate with time for solid specimens tested on 74mm SHPB at different impact velocities

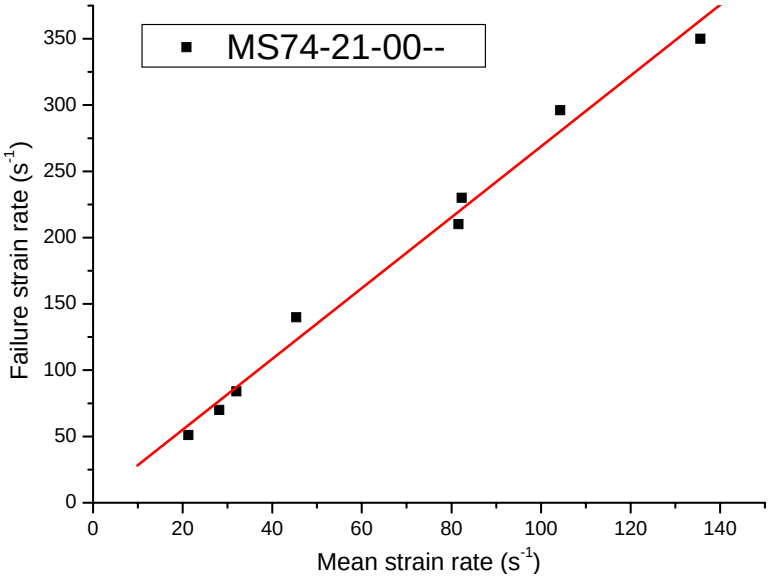

Fig.8 Correlation between the failure strain-rate and the mean strain-rate for 74mm SHPB tests on solid specimens

The axial strain acceleration is defined by

$$\ddot{\varepsilon} = \frac{d\dot{\varepsilon}}{dt} \tag{5}$$

Although the axial strain acceleration is not a constant during the loading period, its variation with time near the failure point is very small, and therefore, the representative axial strain acceleration in the following discussion is determined as the mean value of the axial strain acceleration over the time duration of $10\,\mu s$ before the failure point on the strain-rate curve. It is found that the representative axial strain acceleration increases with the strain-rate at the failure point, as shown in Figs.9 to 11 where variations of the axial strain acceleration with strain-rate are given for solid and tubular SHPB specimens with 37mm, 50mm and 74mm outer diameters, respectively.

It is shown that axial strain acceleration increases with the increase of strain-rate. Axial strain acceleration is related to the accelerated radial expansion (i.e. the radial inertia) of the specimen material, which introduces the radial stress distribution (i.e. the radial confinement) in the cylindrical specimen. Figures 9-11 indicate that the axial strain acceleration is almost independent of specimen type, i.e. whether the specimen is tubular or solid, for a given diameter of the SHPB specimen. However, due to the existence of the free inner surface in the tubular specimen, the radial confinement in the tubular specimen introduced by the axial strain acceleration is less that that in a solid SHPB specimen for a given specimen diameter.

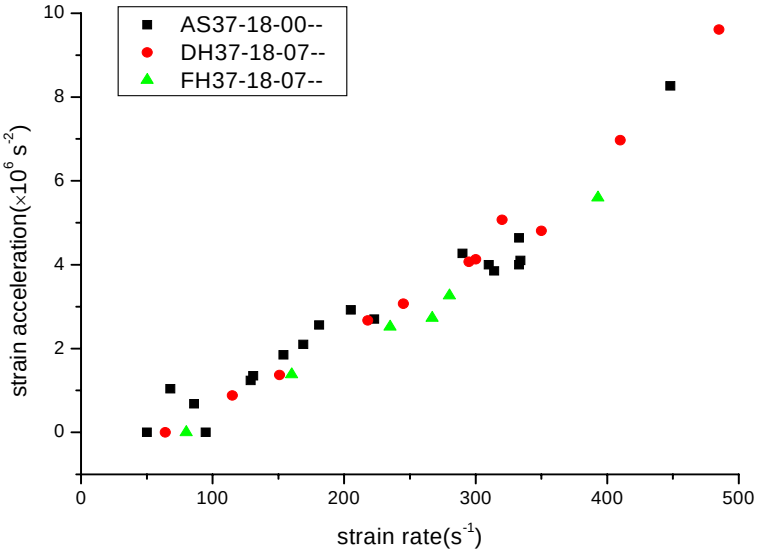

Fig.9 Correlations between the axial strain acceleration and strain-rate in solid and tubular SHPB specimens with 37mm outer diameter.

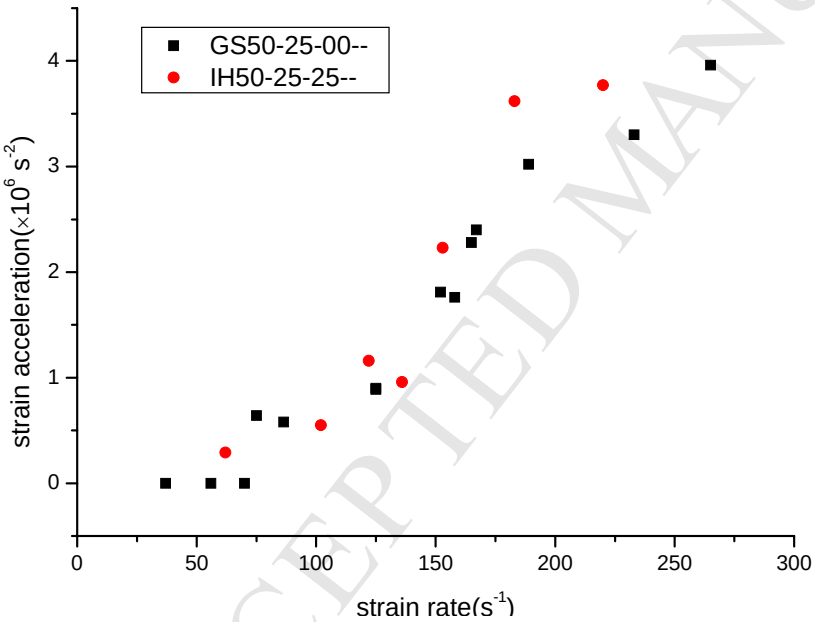

Fig.10 Correlation between the axial strain acceleration and strain-rate in solid and tubular specimens with 50mm outer diameter.

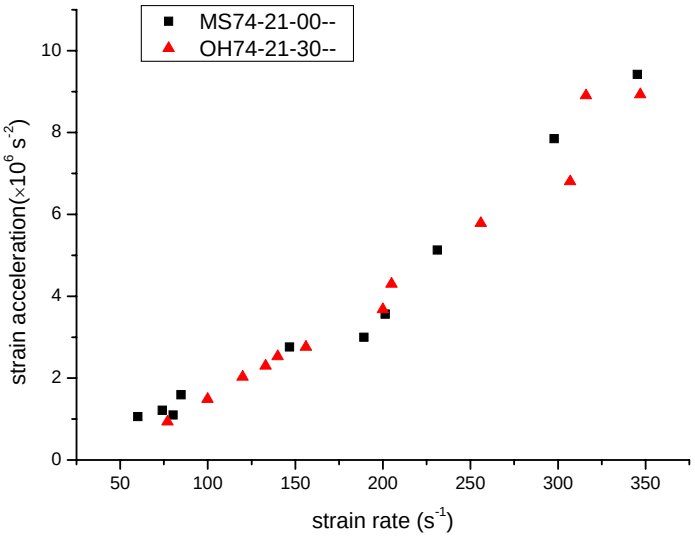

Fig.11 Correlations between the axial strain acceleration and strain-rate in solid and tubular specimens with 74mm outer diameter.

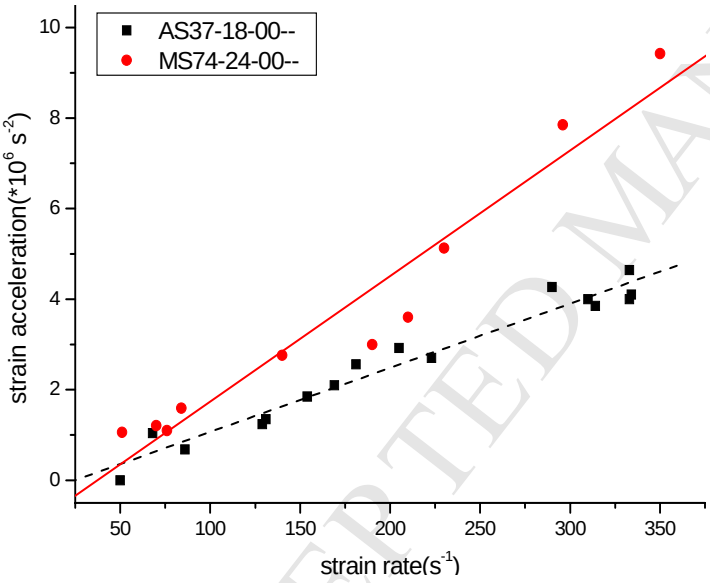

Fig.12 Correlations between the axial strain acceleration and strain-rate in solid specimens with 37mm and 74mm outer diameters

Figure 12 gives the axial strain acceleration in solid specimens with different diameters. It is shown that the axial strain acceleration in specimens with a large diameter is greater than that in specimens with a small diameter.

Therefore, in SHPB tests, it is expected that the DIF from tests on tubular specimens is less than that from solid specimens while the DIF from tests on solid specimens with small diameter is less that that from solid specimens with a large diameter. This will be discussed in Section 3.2.

3.2 About dynamic increase factor (DIF)

3.2.1 DIFs for solid and tubular specimens

Figures 13 to 15 give the variation of DIF with strain-rate for solid and tubular specimens with outer diameters of 37mm, 50mm and 74mm. The data is presented using both logarithmic and linear scales. It shows that the DIFs from SHPB tests on solid specimens are consistently larger than those from SHPB tests on tubular specimens when they have same outer diameter. This becomes more significant when strain-rate is increased. The dependence of the SHPB test results on the dimensions of the specimen observed in this study can be explained qualitatively by inertia-induced radial confinement, which is reported quantitatively in the companion paper by Li et al.(2008).

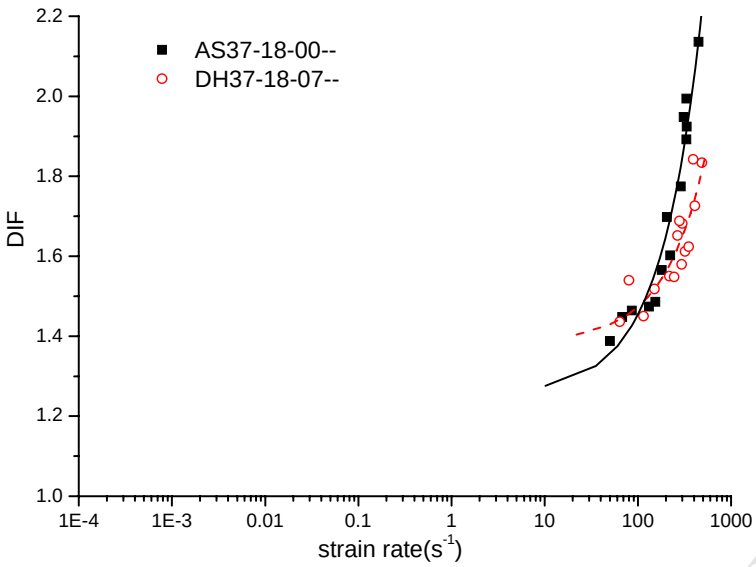

(a)

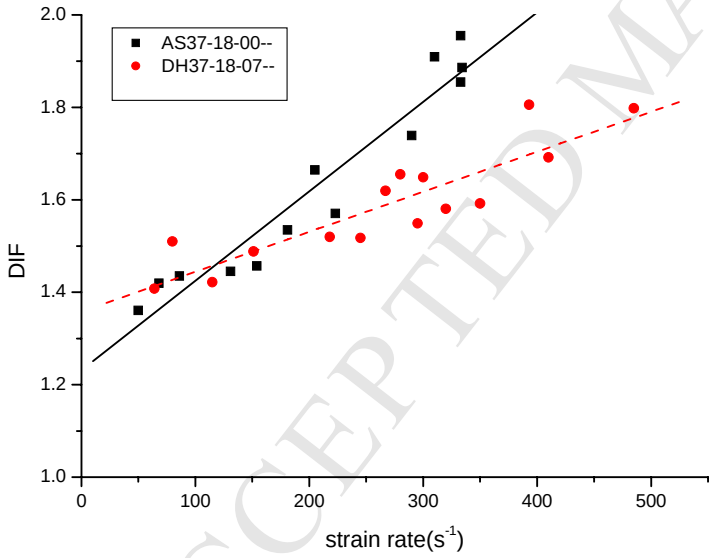

(b)

Fig.13 Variation of DIF with strain-rate for 37mm solid and tubular specimens
(a) strain-rate with logarithm scale, (b) strain-rate with linear scale

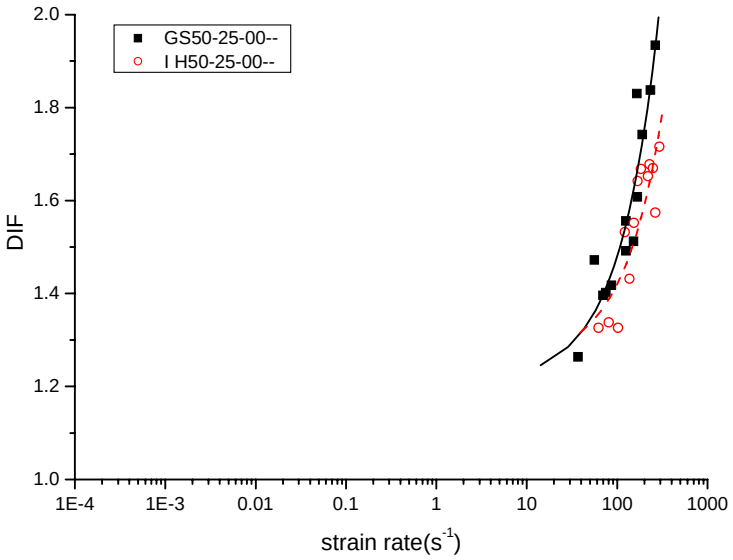

(a)

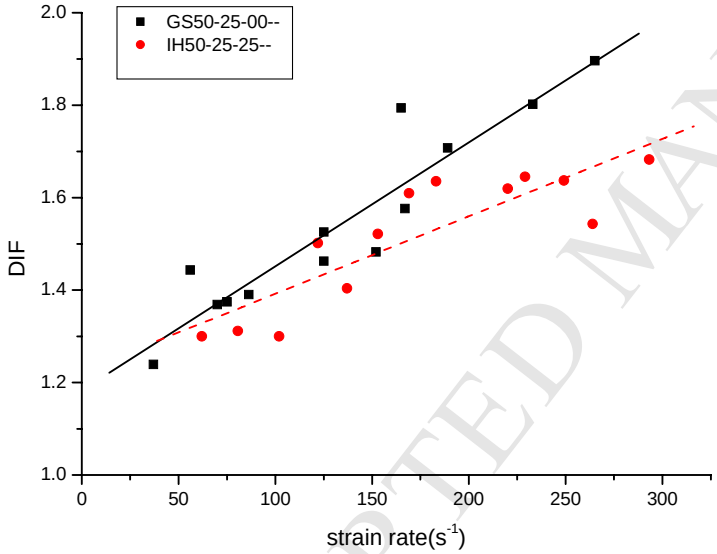

(b)

Fig.14 Variation of DIF with strain-rate for 50mm solid and tubular specimens
(a) strain-rate with logarithm scale, (b) strain-rate with linear scale

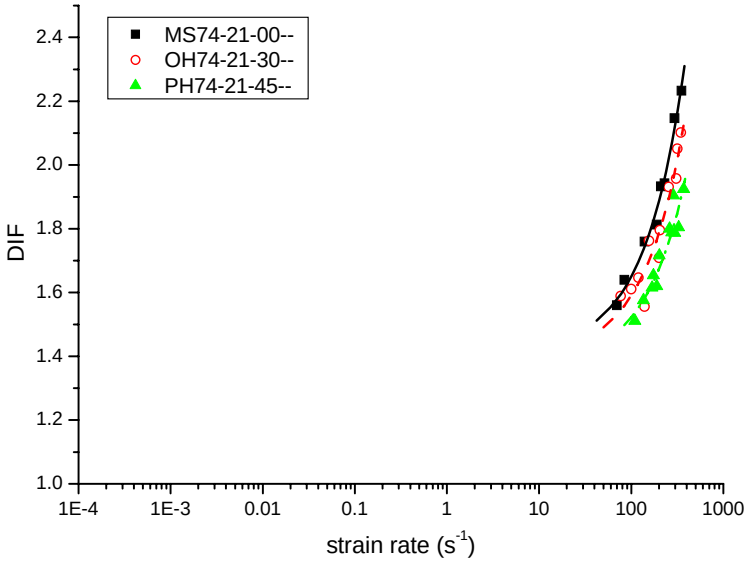

(a)

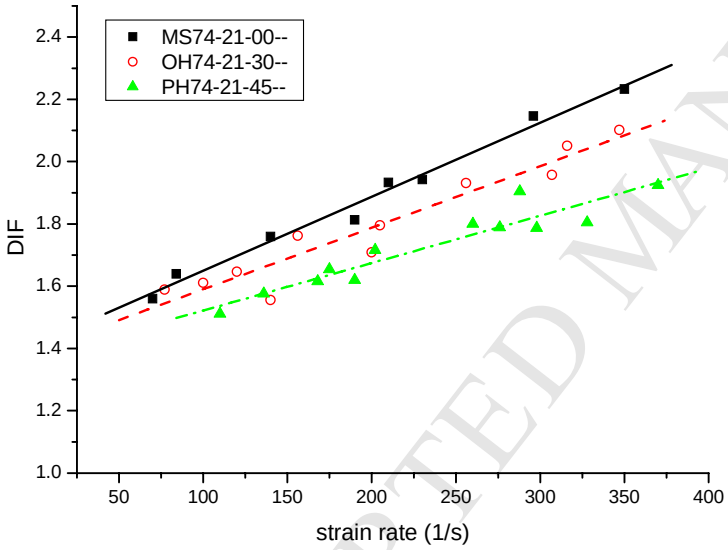

(b)

Fig.15 Variation of DIF with strain-rate for 74mm solid and tubular specimens

(a) strain-rate with logarithm scale, (b) strain-rate with linear scale DIF

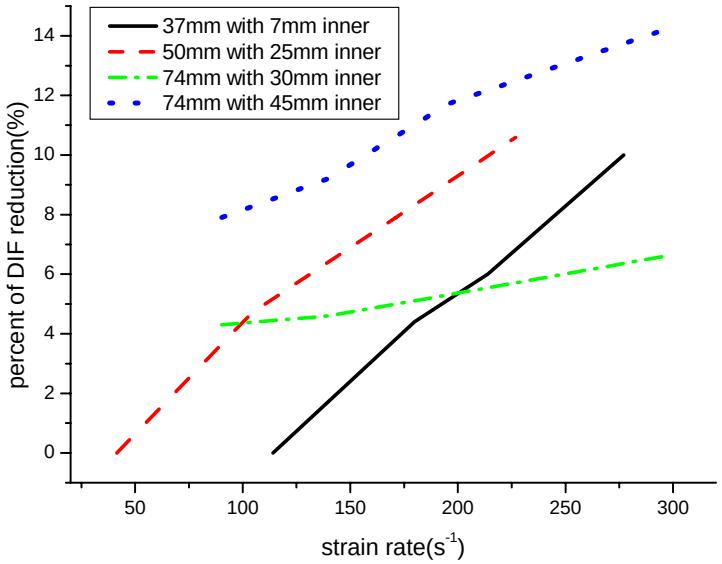

Fig.16 Percentage reduction of DIF

Figure 16 shows the variation of the percentage reduction of DIF with strain-rate for different series of SHPB tests where the percentage reduction of DIF for SHPB specimens with a given outer diameter is defined as $\left(DIF_{solid} - DIF_{tubular}\right)/DIF_{solid} \times 100$. It is shown that the percentage reduction of DIF increases with strain-rate consistently. When the outer diameter of the SHPB specimen is 74mm, the percentage reduction of DIF for specimens with larger inner diameter (i.e. 45mm) is much greater than that for specimens with smaller inner diameter (i.e. 30mm).

3.3 Discussion

Figure 17 compares DIFs of different concrete-like materials from other SHPB tests. Since DIF is a non-dimensional quantity, the dependencies of DIF on strain-rate in Fig.17 do not show obvious differences for different concrete-like materials. However, the influence of the specimen diameter on the DIF of the tested material still exists, as shown in Fig.17, i.e. DIFs obtained for specimens with larger diameter are consistently greater than those obtained for specimens with smaller diameters.

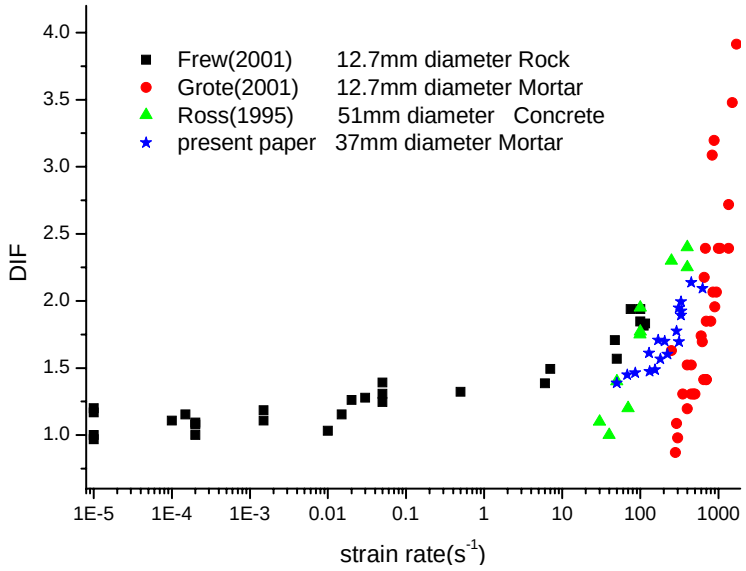

Fig.17 DIFs of concrete-like materials obtained for different diameters of SHPB specimens

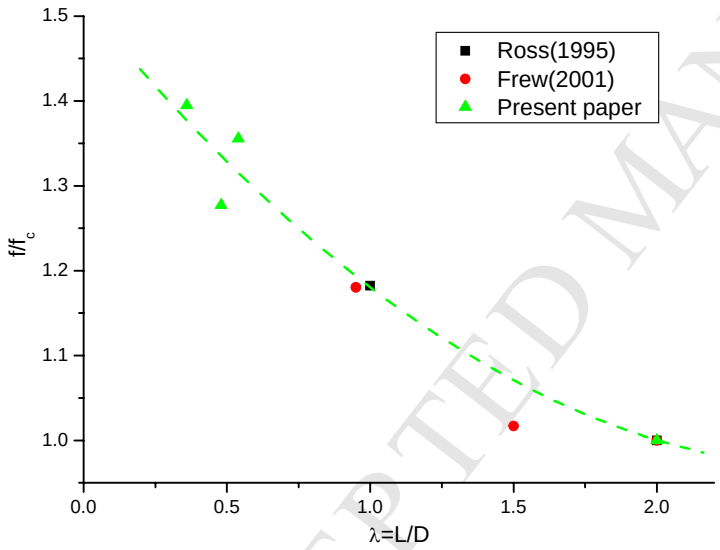

Fig.18 Variation of the normalized quasi-static compressive strength with the length-diameter ratio of the specimen in different experiments.

Another issue which may need further discussion is the effect of the length-diameter ratio ($\lambda = L/D$) on the uniaxial compressive strength of concrete-like materials. Figure 18 clearly demonstrates such an effect in quasi-static compressive tests, which supports the requirement of λ=2.0 in standard quasi-static uniaxial compressive test. In most SHPB tests, the range of λ is between 0.3 and 1.0, which inevitably will contribute to the increase of the radial confinement in the tested specimen. The factors which may influence the dynamic enhancement of the

compressive strength of a concrete-like material include the length-diameter ratio, the diameter of the specimen, axial strain acceleration and the friction on the end surfaces of the specimen in addition to the possible existence of the real strain-rate sensitivity of the concrete-like material. With the decrease of length-diameter ratio, the stress state in the specimen will be changed from uniaxial stress state to uniaxial strain state. Bischoff and Perry (1991) also commented that the height-width ratio of the specimen as well as its overall size could affect the crack pattern by influencing end boundary effects and thus affect the maximum strength and deformability of the tested specimen. Meng and Li (2003) investigated the effect of frictional coefficient by numerical simulation and showed that the coefficient of friction has greater influence on the lateral constrains for a shorter specimen than a longer specimen. Further investigations on the DIF in concrete-like materials will be presented in a companion paper by Li et al.(2009) based on numerical simulation.

5. Conclusions

A series of experiments of solid and tubular cylindrical mortar specimens were performed in a SHPB system. Correlations between the axial strain acceleration and strain-rate are established and related to the influence of radial confinement on DIF of the concrete-like materials. It shows that the DIF of concrete-like materials may be greatly enhanced by the inertia-induced radial confinement, which is unavoidable in many SHPB tests on brittle specimens. Therefore, it is necessary to conduct corresponding numerical simulations to correct the pseudo strain-rate effects on DIF obtained from SHPB measurements. These conclusions are applicable to concrete-like materials in the range of strain-rate between 10^0 and 10^3 $s^{-1.}$

Acknowledgements: This project is supported by the open funding programme (KFJJ05-3) from State Key Laboratory of Explosion Science and Technology. Third author thanks for leave of absence from the School of Mechanical, Aerospace and Civil Engineering at The University of Manchester.

References

Barpi F. (2004), Impact behaviour of concrete: a computational approach, Engineering Fracture Mechanics 71, 2197-2213

Bischoff, P.H., Perry, S.H., 1991.Compression behavior of concrete at high strain-rates. Mater. Struct. 24, 425–450.

Brace W.F., Jones A.H., 1971, Comparison of uniaxial deformation in shock and static loading of three rocks. J. Geophys. Res. 76, 4913-4921.

Comite Euro-International du Beton, 1993. CEB-FIP model code 1990, Redwood Books, Trowbridge, Wiltshire, UK.

Davies E.D.H., Hunter S.C.(1963), The dynamic compression testing of solids by the method of the split Hopkinson bar, J. Mech. Phys. Solids, 11, 155-179.

Donze FV, Magnier SA, Daudeville L, Mariotti C, Davenne L(1999), Numerical study of compressive behaviour of concrete at high strain rates, ASCE J of Engng. Mechanics, 125(10), 1154-1163.

Follansbee P.S., Frantz C. (1983), Wave propagation in the split Hopkinson pressure bar, Journal of Engineering Materials and Technology, 105, 61-66.

Forrestal MJ, Wright TW, Chen W (2007), The effect of radial inertia on brittle samples during the split Hopkinson pressure bar test, Int. J. of Impact Engng., 34(3), 405-411.

Frew DJ, Forrestal MJ and Chen W (2001), A split Hopkinson pressure bar technique to determine compressive stress-strain data for rock materials. Experimental Mechanics, Vol. 41, No.1, 40-46.

Frew DJ, Forrestal MJ and Chen W (2002), Pulse shaping techniques for testing brittle materials with a split Hopkinson pressure bar. Experimental mechanics, Vol. 42, No.1, 93-106.

Gong J.C., Malvern L.E., Jenkins D.A. (1990), Dispersion Investigation in the Split Hopkinson Pressure Bar. Journal of Engineering Materials and Technology, 112, 309-314.

Gorham D.A., Pope P.H., Cox O. (1984), Sources of error in very high strain rate compression tests. Inst. Phys. Conf. Ser. No.70, 151-158.

Gorham D.A. (1989), Specimen inertia in high strain-rate compression. J. Phys. D: Appl. Phys. 22 1888-1893.

Gorham D.A. (1991), An effect of specimen size in the high strain rate compression test. Colloque C3, Suppl. Au Journal de Physique III, Vol.1,411-418

Gorham D.A., Pope P.H. and Field J.E. (1992), An improved method for compressive stress-strain measurements at very high strain rates. Proc. R. Soc. Lond. A 438, 153-170.

Grote D.L., Park S.W. Zhou M. (2001), Dynamic behavior of concrete at high strain rate and pressure: I. experimental characterization. Int. J. of Impact Engng., 25, 869-886.

Gray III, G.T. (2000), Classic split-Hopkinson pressure bar testing, ASM Handbook, 8: Mechanical Testing and Evaluation. ed. H. Kuhn and D.Medlin, publ. Materials Park, Ohio, ASM International, 462-476.

Huang, C., Subhash, G., Vitton, S.J., 2002. A dynamic damage growth model for uniaxial compressive response of rock aggregates. Mech. Mater. 34, 267−277.

Huang, C., Subhash, G., Vitton, S.J., 2003. Influence of lateral confinement on dynamic damage evolution during uniaxial compressive response of brittle solids. J. Mech. Phys. Solids. Vol 51, 1089-1105.

Katayama M, Itoh M, Tamura S, Beppu M, Ohno T, (2007). Numerical analysis method for the RC and geological structures subjected to extreme loading by energetic materials. Int. J. Impact Engng, 34, 1546-1561

Kolsky H (1949), An investigation of the mechanical properties of materials at very high rates of loading, Proc. Phys. Soc. London (B), 62(359), 676-700.

Kotsovos, M.D.,(1987), Consideration of triaxial stress conditions in design: a necessity. ACI J. 84(3), 266-273.

Li QM, Meng H(2003), About the dynamic strength enhancement of concrete-like materials in a split Hopkinson pressure bar test, Int. J. of Solids and Struct., 40, 343-360.

Li QM, Lu YB, Meng H(2009), Further investigation on the dynamic compressive strength enhancement of concrete-like materials based on split Hopkinson pressure bar tests, Part II: Numerical simulations, submitted to Int. J. of Impact Engng..

Meng H, Li QM (2003), Correlation between the accuracy of a SHPB test and stress uniformity based on numerical experiments, Int. J. of Impact Engng., 28(5), 537-555.

Polanco-Loria M, Hopperstad OS, Børvik T and Berstad T, (2008) Numerical predictions of ballistic limits for concrete slabs using a modified version of the HJC concrete model, Int. J. of Impact Engng. 35, 290-303.

Ross, C.A., Thompson, P.Y., Tedesco, J.W., 1989, Split-Hopkinson pressure-bar tests on concrete and mortar in tension and compression, ACI Mater. J. 86, 475–481.

Ross, A., Tedesco, J.W., Kuennen, S.T., 1995. Effects of strain rate on concrete strength. ACI Mater. J. 92 (1), 37–47.

Ross, A., Jerome, D.M., Tedesco, J.W., Hughes, M.L., 1996. Moisture and strain rate effects on concrete strength. ACI Mater. J. 93 (3), 293–300.

Tedesco, J.W., Ross, C.A., 1998, Strain-rate-dependent constitutive equations for concrete, ASME J. Press. Vessel Technol. 120, 398–405.

Tham CY. (2006), Numerical and empirical approach in predicting the penetration of a concrete target by an ogive-nosed projectile. Finite Elements in Analysis and Design. 42, 1258-1268.

Weinong Chen and G. Ravichandran (1997), Dynamic compressive failure of a glass ceramic under lateral confinement. J. Mech. Phys. Solids, Vol 45, No.8, 1303-1328.